



# Contrast Agents in Cardiovascular Magnetic Resonance Imaging

8

David J. Murphy and Raymond Y. Kwong

## Introduction

The inception of the era of magnetic resonance imaging (MRI) has transformed modern cardiovascular imaging. Since Damadian et al. manufactured the first whole-body MRI machine capable of imaging the human body in 1977 [1], continued advances in MRI technology have placed it at the forefront of noninvasive cardiovascular imaging. MRI provides reproducible, multi-parametric, multi-planar two-dimensional (2D), and three-dimensional (3D) imaging with high temporal and spatial resolution. MRI has an advantage over other noninvasive cardiovascular imaging modalities, as it does not expose the patient to ionizing radiation. It offers excellent soft tissue contrast, which can be further enhanced by the use of paramagnetic MR contrast agents, improving both the signal-to-noise (SNR) and contrast-to-noise (CNR) ratios.

## General Considerations in MRI Contrast

### Image Contrast

One of the principal advantages of MRI over other diagnostic imaging modalities is its superior soft tissue contrast. Image contrast in MRI refers to relative differences in signal intensity (SI) between different tissues, allowing for their differentiation by the reader on the MR image. Contrast exists between different tissues due to differences in proton density

(the number of “MRI visible” protons per unit volume), inflow phenomena, susceptibility, and the tissue relaxation time. MRI pulse sequences are designed to emphasize these differences in signal intensity in order to provide images of diagnostic quality.

### T1 and T2 Tissue Relaxation

When the human body is placed in the MRI magnet, protons in the body will precess in the strong magnetic field. The protons will align in the longitudinal direction of the external magnetic field ( $B_0$ ). Each proton has a longitudinal vector pointing either with the external field (low-energy protons) or against the field (high-energy protons). Due to the small excess amount of low-energy protons, the resultant vector is a steady longitudinal magnetization along the direction of  $B_0$ , the magnitude of which is proportional to the strength of the external magnetic field, measured in teslas (T). There is no resultant vector in the transverse direction, as the individual protons point in random directions, canceling each other out. When an external radiofrequency (RF) pulse is applied, this has two effects. Some of the protons are excited to the high-energy state, pointing against the longitudinal magnetic field, and the spins get in phase in the transverse plane. This results in an overall reduction in the longitudinal magnetization vector, and an increased horizontal magnetization vector. Once the RF pulse is turned off, the higher-energy protons lose their energy and flip back to their low-energy orientation along the direction of  $B_0$ . This process, by which high-energy spins dissipate their energy and transform back to the lower-energy state, is called T1 or spin-lattice relaxation. This transfer occurs when a tissue encounters a magnetic field fluctuating close to its Larmor frequency, which is in turn dependent of the strength of  $B_0$ . The T1 relaxation time depends on the net transfer of energy from the spin to its surrounding environment (“lattice”), hence the term spin-lattice relaxation. As spin-lattice relaxation occurs, the longitudinal magnetization

D. J. Murphy  
Non-invasive Cardiovascular Imaging, Radiology Division,  
Department of Radiology, Brigham and Women’s Hospital,  
Boston, MA, USA

R. Y. Kwong (✉)  
Non-invasive Cardiovascular Imaging, Cardiovascular Division,  
Department of Medicine, Brigham and Women’s Hospital, Harvard  
Medical School, Boston, MA, USA  
e-mail: rykwong@bwh.harvard.edu

component recovers in an exponential fashion. T1 is the length of time it takes for the longitudinal magnetization of a tissue to recover to 63% of its original value. T1 times vary between different tissues and among tissues in different magnetic field strengths, providing tissue contrast. Tissues with shorter T1 times have higher SI on T1-weighted images following each RF pulse.

After application of the RF pulse, the spins precess in phase in the transverse plane, resulting in an overall net transverse magnetization vector. Small local differences in the local magnetic field strength cause the spins to rotate at a slightly different rate, driving them out of phase. This process is called T2 or “spin-spin” relaxation. The transverse magnetization component of a tissue decays in an exponential fashion to its original zero value. The T2 value for a given tissue is the length of time it takes to reduce the magnetization by 63% of its peak value. T2 relaxation time is strongly influenced by the local tissue environment. Inhomogeneities in the local magnetic field (B1) drive faster local spin dephasing, resulting in a faster decay of transverse signal, referred to as T2\* relaxation.

## Relaxivity

MRI contrast agents improve image contrast by shortening tissue T1 and T2 relaxation times. Paramagnetic contrast agents shorten T1 and T2 relaxation times of water protons in their immediate surroundings, creating a locally increased magnetic field strength. This change in the local magnetic field strength results in increased local field inhomogeneities, driving the shortening of T1 and T2 relaxation. The resultant increased SI on T1-weighted images provides the basis behind the use of contrast agents in MR. The degree to which a contrast agent shortens T1 and T2 is referred to as relaxivity. This is the inverse of T1 and T2 and is expressed as R1 (s<sup>-1</sup>) and R2 (s<sup>-1</sup>), respectively. The increase in R1 or R2 after administration of a given concentration of contrast medium (C, mmol/L) is the relaxivity constant of that agent, denoted as r1 (mM<sup>-1</sup> s<sup>-1</sup>) and r2 (mM<sup>-1</sup> s<sup>-1</sup>), respectively.

$$R1 = 1/T1 = r1 \times C$$

$$R2 = 1/T2 = r2 \times C$$

As the concentration of the contrast agent (C) increases, this increases relaxivity, thus shortening T1, resulting in higher SI on T1-weighted imaging. This does not come without consequences though; T2 is also shortened resulting in lower SI on all MR images, including those with T1 weighting.

## Paramagnetic Metals

Paramagnetic metals function as effective MR contrast agents due to their ability to add to the local magnetic field.

They shorten both T1 and T2 relaxation times, but it is the former effect that is the most useful in clinical imaging, increasing SI on T1-weighted images. All of the lanthanide (rare-earth) metals with unpaired electrons have potential to be paramagnetic agents; however, most of these agents are not suitable for clinical MRI due to their unmatched metal spin relaxation time and Larmor frequency [2]. Those rare-earth metals with suitable characteristics for MRI include gadolinium (Gd<sup>3+</sup>), manganese (Mn<sup>2+</sup>), iron (Fe<sup>3+</sup>), and dysprosium (Dy<sup>3+</sup>) [3]. Initial studies in the 1980s explored the use of manganese (Mn<sup>2+</sup>) [4] and iron (Fe<sup>3+</sup>) [5]-based contrast agents, before a German group, led by Weinmann et al., demonstrated that gadolinium (Gd<sup>3+</sup>) was an effective paramagnetic ion in terms of T1 relaxivity [6, 7].

## Gadolinium

Gadolinium does not produce MRI signal by itself; it achieves this by altering the surrounding magnetic field. The Gd<sup>3+</sup> ion has seven unpaired electrons, each of which contributes to a strong magnetic moment, and an unusually strong hydrogen-proton spin-lattice relaxation effect. This makes it an ideal paramagnetic contrast agent. The magnetic moment ( $\mu$ ) of each unpaired electron is over 600 times greater than that of a proton [8]. The T1 relaxation time is proportional to the square of the magnetic moment ( $\mu^2$ ); the presence of Gd<sup>3+</sup> causes protons nearby to relax a million times faster than usual, resulting in increased T1 SI. The Gd<sup>3+</sup> ion itself is highly toxic; therefore, they are chelated with organic ligands to create gadolinium-based contrast agents (GBCAs) that can be used safely in clinical imaging.

The performance of a contrast agent is highly dependent on its concentration and its relaxivity constant, a numerical expression of the extent to which it shortens T1 and T2 relaxation times in a given magnetic field strength. The relationship between signal intensity and gadolinium concentration is however not linear. At higher concentrations, its T2 shortening effect can overcome the T1 shortening causing signal loss, even in T1-weighted images. This is the main reason why MRI SI is not directly proportional to the concentration of gadolinium, and why beyond a certain concentration, signal loss can occur. This effect can be observed in routine clinical practice as localized signal loss in areas with high gadolinium concentrations, such as in the urinary bladder, renal collecting systems, and the veins adjacent to the injection site.

## Super-Paramagnetic Agents

Super-paramagnetic agents are another group of rare-earth metals that can be used as MR contrast agents. They form a significantly larger magnetic moment than the paramagnetic agents such as gadolinium. This larger magnetic moment has a substantially greater effect on shortening T2 rather than T1

relaxation times, causing areas of reduced SI on T2-weighted imaging. These agents are made of an iron oxide core or iron/manganese composite, covered in a polymer matrix.

## Gadolinium-Based Contrast Agents (GBCAs)

### Basic Structure

All of the gadolinium-based contrast agents (GBCAs) contain the paramagnetic gadolinium ion,  $Gd^{3+}$ . It is complexed with a ligand or chelator to protect against the potential toxic effects of the free  $Gd^{3+}$  ion. The free  $Gd^{3+}$  ion is highly toxic and can competitively inhibit calcium ( $Ca^{2+}$ ) ions, which can adversely affect enzyme activity and voltage-gated calcium channels [9]. The presence of a chelator protects the endogenous tissue from interacting with the toxic  $Gd^{3+}$  ions and allows the agent to be excreted from the body without undergoing significant biotransformation. In order to prevent dissociation of free  $Gd^{3+}$  ions from the GBCA in vivo, the chelator must be powerful [10]. The presence of the chelator does hinder the paramagnetic effect of the  $Gd^{3+}$  ions, reducing the overall relaxivity of GBCAs [11]. Despite the presence of a chelator, no GBCA is completely resistant to dissociation of free  $Gd^{3+}$  ions. It is important, therefore, that GBCAs are rapidly cleared from the body after injection and imaging to prevent accumulation of a potentially toxic agent. Currently available GBCAs are largely cleared by either renal or hepatobiliary excretion, depending on the individual agent.

There are currently nine available GBCAs licensed by the European Medicines Agency (EMA) and the Food and Drug Administration (FDA) in the USA for clinical use. The properties of the common GBCAs are summarized in Table 8.1. These different agents can be classified according to their chemical structure. The chelating ligands are either linear or macrocyclic in structure, and the overall GBCA structure is either ionic (possessing a charge) or nonionic (neutral). In the linear agents, the ligand wraps around the  $Gd^{3+}$  ion, but does not completely enclose it. The macrocyclic agents consist of a chelator, which completely surrounds the  $Gd^{3+}$  ion in a cage-like structure. The latter agents demonstrate greater stability in vivo than the linear agents, with little (if any) free  $Gd^{3+}$  ion dissociation, even in patients with significant renal impairment [12]. The  $Gd^{3+}$  ion has nine coordination sites; eight are used as bonds between the  $Gd^{3+}$  ion and its chelator, with the single remaining site of importance in the GBCA's primary function as a paramagnetic agent and its interaction with surrounding water molecules [13]. The ionic linear GBCAs (gadopentetate dimeglumine (Gd-DTPA), gadoxetate disodium (Gd-EOB-DTPA), gadofosveset trisodium (Gd-DTPA-DO3A)) each have an overall negative charge due to five ionic carboxylic oxygen-binding atoms (each with one negative charge) and three neutral amino nitrogen atoms binding with the  $Gd^{3+}$  ion. This overall negative charge is neutralized by the addition of either a sugar amine with a positive charge

(meglumine) or sodium ( $Na^+$ ) ion. The nonionic linear GBCA (gadodiamide (GD-DTBA-BMA), gadoversetamide (Gd-DTPA-BMEA)) ligands bind the  $Gd^{3+}$  ion with three carboxylic oxygen-binding atoms, two nonionic carboxylic oxygen-binding atoms, and three neutral amino nitrogen atoms. This results in no overall charge, but the bond between the  $Gd^{3+}$  ion and chelator is weaker than in the linear ionic compounds, decreasing the stability of the linear nonionic compounds.

The macrocyclic GBCAs are derived from a macrocyclic polyamino ring, with a greater inherent stability compared with their linear counterparts. The macrocyclic GBCAs can be divided into ionic and nonionic agents, based on the number of ionic carboxylic oxygen atoms in the chelator; those with more than three will have an overall negative charge. Both the ionic macrocyclic GBCA (gadoterate meglumine (Gd-DOTA)) and nonionic GBCAs (gadobutrol (Gd-BT-DO3A), gadoteridol (Gd-HP-DO3A)) are inherently stable. The nonionic macrocyclic GBCAs have a lower osmolality and viscosity than the ionic macrocyclic agents [13].

### Stability

The stability of GBCAs can be described with reference to the concepts of thermodynamic and kinetic stability. Thermodynamic stability is the energy required to break the bonds between the  $Gd^{3+}$  ion and its chelator, resulting in release of the free  $Gd^{3+}$  ion. Kinetic stability is the rate at which this dissociation occurs. These properties depend on a number of factors, including the inherent structure of the agent (macrocyclic vs linear, strength of ionic bonds present) and the surrounding environment (temperature and pH). For clinically available GBCAs, the ligand structure, be it macrocyclic or linear, is the most important variable in determining dissociation kinetics. This is due to the requirement for multiple bonds to be simultaneously broken for the  $Gd^{3+}$  ion to break free from a macrocyclic ligand, whereas the  $Gd^{3+}$  ion can break free from the linear ligands one bond at a time, akin to opening a zip on an item of clothing. This results in the macrocyclic agents having a higher kinetic stability compared to their linear counterparts [14]. In addition, linear GBCAs are more susceptible to competitive reactions between endogenous cations, such as copper ( $Cu^{2+}$ ) and zinc ( $Zn^{2+}$ ), and the ligand resulting in  $Gd^{3+}$  dissociation [15]. The dissociation half-life of GBCAs are reported as kinetic stability in acidic conditions (pH 1.0), because the dissociation rates at physiological conditions (pH 7.4) are too slow to accurately measure [10, 16].

### Osmolality

The majority of GBCAs are formulated at 0.5 M (mol/L). This allows for rapid administration, and by consequence they are somewhat hyperosmolar relative to plasma. Agents

**Table 8.1** Summary table of gadolinium-based contrast agent's properties [8]

Class	Charge	Chemical name	Abbreviation	Trade name	Concentration (mol/L)	Relaxivity (L/mmol s) (3T in plasma)	Osmolality (mOsm/kg H <sub>2</sub> O, 37°C)	Excretion	Conditional complex stability, log K <sub>cond</sub>	NSF risk
Linear	Nonionic	Gadodiamide	Gd-DTPA-BMA	OmniScan (GE Healthcare)	0.5	4.0	789	Renal	14.9	High
		Gadoversetamide	Gd-DTPA-BMEA	OptiMARK (Mallinckrodt)	0.5	4.5	1110	Renal	15.0	High
		Gadopentetate dimeglumine	Gd-DTPA	Magnevist (Bayer)	0.5	3.7	1960	Renal	18.4	High
	Ionic	Gadobenate dimeglumine	Gd-BOPTA	MultiHance (Bracco)	0.5	5.5	1970	Renal (95% HPB (5%))	18.4	Intermediate
		Gadoxetate disodium	Gd-EOB-DTPA	Primovist Eovist (Bayer)	0.25	6.2	688	Renal (50% HPB (50%))	18.7	Intermediate
		Gadofosveset trisodium	Gd-DTPA-DO3A	Ablavar (Lantheus)	0.25	9.9	825	Renal (95% HPB (5%))	18.9	Intermediate
Macrocyclic	Nonionic	Gadobutrol	Gd-BT-DO3A	Gadovist Gadavist (Bayer)	1.0	5.0	1603	Renal	15.5	Low
		Gadoteridol	Gd-HP-DO3A	ProHance (Bracco)	0.5	3.7	630	Renal	17.2	Low
	Ionic	Gadoterate meglumine	Gd-DOTA	Dotarem (Guerbet)	0.5	3.5	1350	Renal	19.3	Low

Reprinted from Lohrke et al. [8]

with lower osmolality have improved dose tolerance, which is useful when administering rapid boluses via a power injector. GBCAs with higher osmolality can be problematic in cases of extravasation and can result in local soft tissue necrosis [17, 18].

## Biodistribution and Elimination

The distribution of the various GBCAs throughout the body after administration differs for each agent and is referred to as biodistribution. After intravenous injection, GBCAs first enter the bloodstream. From here, the majority of GBCAs diffuse into the interstitial space (space between cells) from the capillaries, rapidly reaching equilibrium between the intravascular and interstitial compartments. Collectively, these two compartments make up the extracellular compartment. In addition, the GBCA molecules may be taken up by cells in specific organs (liver and kidney) according to their chemical structure; this occurs by both active uptake and passive diffusion. This varying biodistribution of GBCAs allows us to group them accordingly into extracellular, intracellular, tissue-specific and blood pool/intravascular agents [19]. For the majority of commercially available GBCAs, there is no intracellular distribution, except for varying hepatocyte uptake for certain agents (gadoxetate disodium/gadoxetic acid and gadobenate dimeglumine) [20]. In cardiovascular imaging, we focus mainly on the extracellular and intravascular agents, as there are currently no commercially available intracellular GBCAs for cardiovascular purposes.

## Localization of Cardiovascular GBCAs

The clinical benefit of administering contrast agents relies on our ability to localize the agent within a given body compartment. This can be achieved by altering a number of different MRI parameters. After injection of a bolus of contrast agent into a peripheral vein, it travels through the pulmonary circulation first and then into the arterial system. The rapid acquisition of images while the contrast agent is in the arterial system is the cornerstone behind magnetic resonance angiography (MRA). Figure 8.1 shows examples of MRA that use different contrast agents. There are a number of methods that can be employed to appropriately time MRA imaging. One of these methods is the test bolus method. This involves administering 1–2 ml of contrast and acquiring a series of rapid 2D images of the vessel in question to determine optimum imaging time. The diagnostic MRA is then performed using the temporal information garnered from the test bolus. Fluoroscopic triggering is another commonly used technique; this consists of administering the full bolus of contrast and simultaneously obtaining

rapid, fluoroscopic-like images of the area of interest. When the bolus is visually detected within the vessel, the operator can trigger the MRA acquisition. As the contrast bolus enters the venous circulation, it begins to redistribute from the intravascular into the extravascular interstitial space, eventually reaching equilibrium. The proportion of the contrast bolus that leaves the blood pool is inversely related to its avidity of plasma protein binding.

## Extracellular Fluid GBCAs

The majority of GBCAs in routine clinical use are extracellular fluid (ECF) agents. After injection, they initially distribute in the intravascular space, before rapidly diffusing across the vascular membranes into the interstitial space, establishing equilibrium. By using specific pulse sequence parameters, it is possible to image the contrast media in arterial, venous, and equilibrium phases. The arterial phase is the time between contrast arrival in the arterial region of interest and venous filling. The timing of the arterial phase is highly dependent on the patient's cardiac output but is usually between 15 s and 25 s. As the contrast fills the venous system, it diffuses rapidly into the interstitial space across the vascular membranes. The equilibrium, or steady-state, phase occurs after approximately 10 min, as the GBCA concentration reaches equilibrium between the intravascular and interstitial compartments. Tissues with large interstitial spaces and/or leakier capillaries will concentrate more GBCA in this phase, leading to increased SI in these regions during steady-state phase imaging. Figure 8.2 shows examples of cardiac late gadolinium enhancement images using different contrast agents.

ECF GBCAs quickly distribute to the extracellular space after injection and are excreted via glomerular filtration, with a terminal half-life for plasma elimination of 90 min for subjects without renal impairment [11, 19]. As these compounds are exclusively excreted via the kidneys, their rate of elimination slows down in patients with impaired renal function, with a strong correlation between the blood elimination half-life of the agent and creatinine clearance [21, 22].

Binding of GBCA to a protein or other larger molecular structure can slow down the tumbling rate, increasing the relaxivity of the agent. Gadobenate dimeglumine (Gd-BOPTA) and gadoxetate disodium (Gd-EOB-DTPA) both exhibit weak plasma protein binding (approximately 10%) to the presence of an aromatic ring. This weak plasma protein binding helps increase relaxivity compared to the other ECF GBCAs [20, 23, 24]. This plasma protein interaction does not impact significantly on renal clearance rates, and the nature of the plasma protein interaction is too weak and transient for them to act as blood pool agents [19].



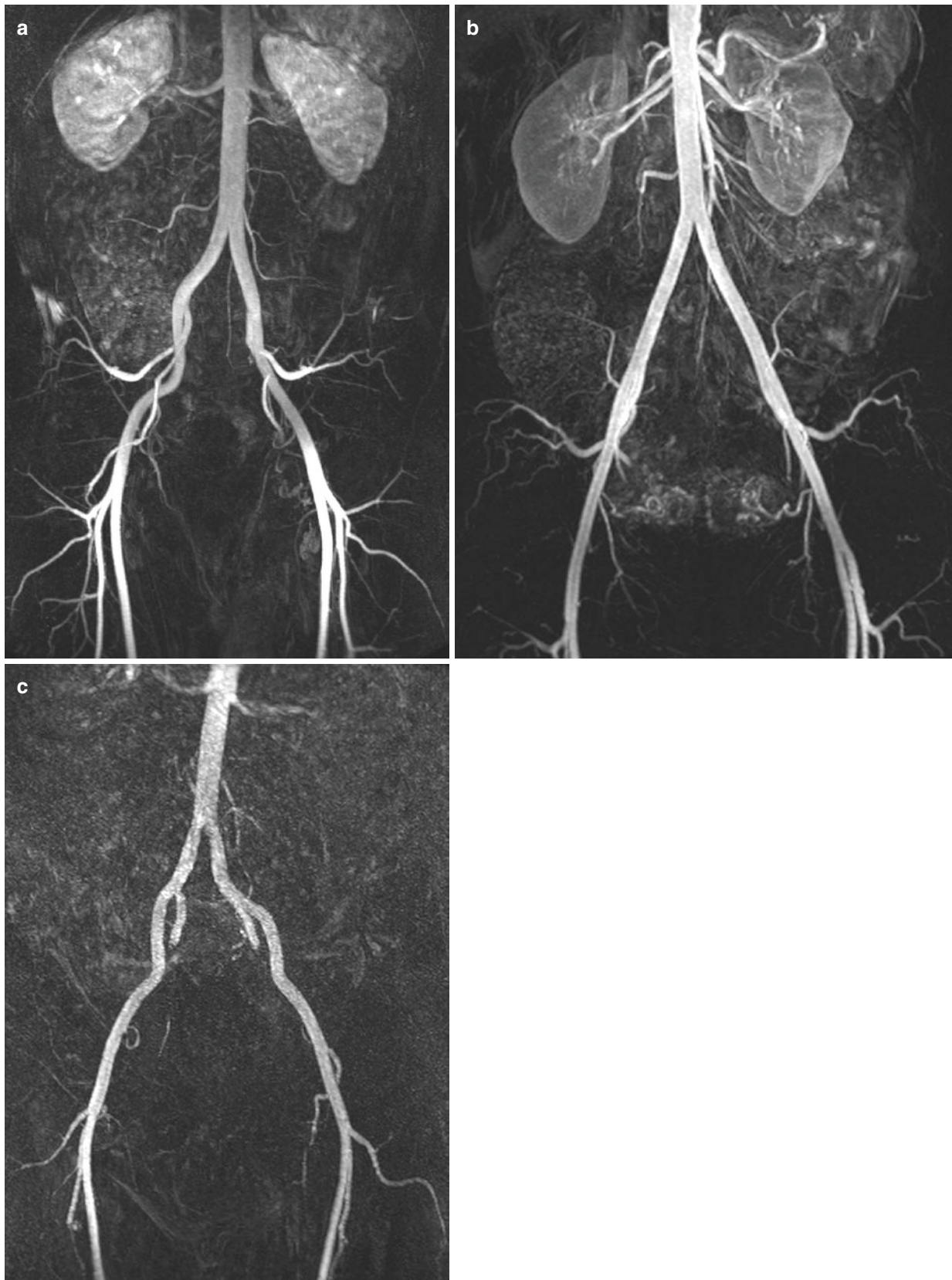


**Fig. 8.1** Coronal, arterial phase subtraction maximum intensity projection (MIP) MR images of the abdomen and pelvis with different contrast agents. (a) Macrocytic ionic GBCA gadoterate meglumine (Dotarem). (b) Linear ionic GBCA gadobenate dimeglumine (MultiHance). (c) USPIO agent ferumoxytol (Feraheme) in a patient

with chronic renal failure. Note that multihance-enhanced images enhanced the vascular lumen substantially stronger than Dotarem given its higher relaxivity. For patients with renal failure who cannot receive GBCAs, ferumoxytol is a viable option as an intravascular contrast agent using T1 weighted MRA methods

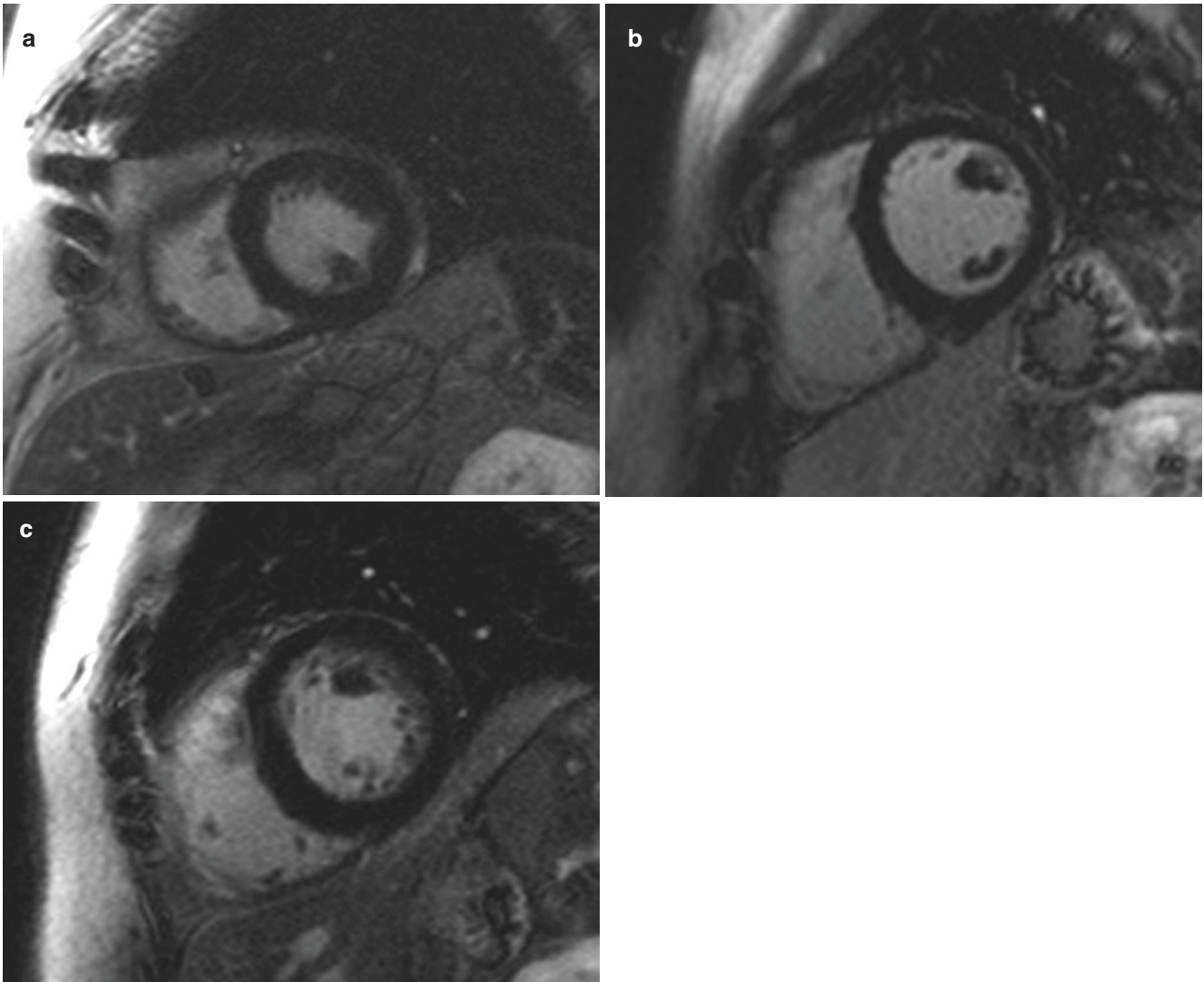


**Fig. 8.2** Cardiac MRI short-axis mid-left ventricle late gadolinium enhancement images with different GBCAs. (a) Linear ionic GBCA gadopentetate dimeglumine (Magnevist). (b) Linear ionic GBCA gadobenate dimeglumine (MultiHance). (c) Macrocyclic ionic GBCA

gadoterate meglumine (Dotarem). Note that on average multihance can provide higher signal-to-noise LGE images, but tissue enhancement may be affected by high protein-binding and it not be consistent with less protein-bound GBCAs

## Intravascular GBCA

Gadofosveset trisodium (Gd-DTPA-DO3A/MS-325) is currently the only intravascular GBCA licensed by the FDA. It was licensed by the European Medicines Agency for distribution in the European Union (EU) in 2005 but was voluntarily withdrawn from commercial use in the EU by the manufacturer in 2011. It is a linear ionic agent, which binds strongly to albumin, limiting its diffusion into the extravascular space [25, 26]. Its strong albumin binding is due to a lipophilic albumin-binding group (biphenylcyclohexyl) on the chelate. The fraction of the agent that binds to plasma albumin depends on both the concentrations of albumin and of the agent itself. The overall effect of this is an increase in plasma relaxivity compared with the extracellular fluid GBCAs. The increased blood SI is appreciable on T1-weighted images up to 4 h post administration [27], with a serum half-life of 2–3 h [28]. Gadofosveset is predominantly renally excreted, but there is a small component (approximately 5%) of biliary excretion [29]. It is not completely confined to the blood pool, with a small proportion diffusing into the interstitial space. Due to its relatively high proportion of albumin binding, it is excreted slower than other GBCAs, with a terminal plasma half-life of 16.5 h in patients with normal renal function, with slower excretion in patients with renal impairment [30]. It has a high kinetic stability compared with the other linear GBCAs, with in vitro testing showing stability two to three times that of Gd-DTPA [31].

## GBCA-Related Imaging Artifacts

Localized signal loss is one of the commonly observed artifacts associated with GBCA use. This primarily occurs in areas of high concentration of the agent and is caused by T2-shortening effect. In areas of high GBCA concentration, the T2 relaxation time is shortened to such an extent that it is less than the echo time (TE), resulting in localized signal loss, even on T1-weighted imaging. This effect can be observed in extravascular locations of high GBCA concentration, such as the renal collecting systems and urinary bladder. It can be relevant in cardiovascular imaging when performing venous extremity imaging, particularly of the upper limb, where injection of the limb in question should be avoided, where possible.

During first-pass imaging with GBCAs, the bolus increases the magnetic field within the capillaries. Tissues with a high capillary density experience a greater local change in magnetic field, creating a gradient in the local magnetic field between the capillaries and adjacent tissue. This gradient increases local field ( $B_1$ ) inhomogeneity,

increasing tissue T2\*, causing signal loss on susceptibility-weighted imaging. This T2\* effect can be used in clinical myocardial perfusion MR [32, 33].

## Future GBCAs

There are several novel GBCAs currently under investigation for possible clinical use. Among them are agents with substantially higher longitudinal relaxivity than those currently commercially available. Increased relaxivity would allow for less GBCA to be used, which may help improve patient safety. GBCAs increase relaxation by creating a local fluctuating magnetic field. The T1 relaxivity of GBCAs depends in part on the number of water molecules bound directly to the Gd<sup>3+</sup> complex. The GBCA complex tumbles in a solution, creating a fluctuating magnetic field, inducing local proton relaxation. The tumbling rate is described by the characteristic rotational time,  $\tau_R$  [34]. The molecular size, complex rigidity, and affinity of protein binding all affect the  $\tau_R$  of the agent. Increasing the rotational correlation time (i.e., slowing the tumbling rate) will increase relaxivity. This can be achieved by making larger molecules, with more protein binding. A number of new agents are being trialed, bound to molecules such as albumin, dextran, and other macromolecules, with up to five times the relaxivity of current approved GBCAs [35]. There is a trade-off with this increase in molecule, as it can limit their distribution throughout the body. This may prove to be advantageous in vascular MRI, but is not desirable for a CMR contrast agent.

---

## GBCA Adverse Reactions

### Allergic-Like Reactions

Adverse reactions to GBCA administration are rare. These can manifest as non-allergic reactions (headache, fatigue, nausea, vomiting, taste disturbance) or allergic-like reactions. Although these adverse reactions can appear allergic in phenotype, their precise mechanism at a cellular level is poorly understood. They do not demonstrate the classic immunoglobulin (IgE)-mediated response typically seen in type 1 hypersensitivity reactions; however, they do manifest clinically as allergic-type reactions [36]. They can be classified as either mild, moderate, or severe according to the clinical severity [37]. Mild reactions manifest as mild pruritus, hives, and limited cutaneous edema. Moderate reactions have more prominent symptoms, such as diffuse erythema and pruritus with stable vital signs. Severe reactions to GBCA are rare and can manifest as respiratory distress, bronchospasm,



hypotension, and anaphylaxis and can ultimately lead to cardiac arrest. The incidence of minor adverse reactions is similar across all the currently available GBCAs [38–40]. A retrospective review of over 150,000 GBCA administrations reported an overall reaction rate of 5.9 per 10,000 injections, 78% of which were classed as mild; the overall rate of severe reactions was 1 per 40,000 GBCA injection [38]. The reported overall frequency of allergic-like reactions to GBCAs of 0.04–0.07% [38, 41] is less than the approximate rate of 1.5% reported for iodinated contrast media used in CT and invasive angiography [42].

Risk factors for allergic-type reactions include asthma, prior allergic-type reaction to contrast media, and prior allergic reaction to substances other than contrast media. Most mild reactions resolve without any treatment, requiring only a period of observation before safe discharge from the radiology department. Anaphylaxis to GBCAs is rare but does occur; a review of the FDA's adverse event reporting system from 1988 to 2012 found 614 reported cases of anaphylaxis associated with GBCAs [43]. Pharmacological therapy for mild reactions consists of oral antihistamine therapy, with steroids and bronchodilators required for more serious reactions [44]. In the rare case of a serious or anaphylactic reaction, prompt treatment with epinephrine is lifesaving.

Most patients who develop an allergic-like reaction after GBCA injection are not precluded from receiving them again in the future. A recurrence rate of allergic-like reactions of approximately 30% was reported on one series of over 140,000 GBCA administrations [45]. This risk of recurrence is reflected in international guidelines. The American College of Radiology (ACR) and the United Kingdom Royal College of Radiologists (RCR) recommend the use of steroid and antihistamine premedication for patients with a history of a moderate or severe reaction prior to readministration [37, 46]. Even with appropriate premedication, breakthrough allergic reactions can occur [47]. There is currently no evidence that steroid and antihistamine premedication reduce the risk of severe contrast reactions. Therefore, the decision to administer GBCA to a patient with a documented history of a severe reaction or anaphylaxis to GBCAs should be made on a case-by-case basis, after an individualized risk-benefit analysis.

## Extravasation

Extravasations occur when the contrast media escapes from the venous lumen into the interstitial space during contrast injection. The incidence of contrast media extravasation can be reduced by a number of simple steps. Intravenous cannulas should be checked that they are appropriate for use prior to contrast administration by the use of a saline flush. The use of a 20-gauge or larger cannula in an antecubital or other

large forearm vein is recommended when flow rates of 3 ml/s or higher are required, and flow rates should not exceed 1.5 ml/s in 22-gauge catheters, or those placed in peripheral locations, such as in the hands [37]. A test injection may be performed when using a power injector, which is commonly used in cardiovascular imaging.

Treatment is usually conservative, involving elevation of the affected limb and application of a warm or cold compress. Severe complications include compartment syndrome, skin ulceration, and tissue necrosis. Most patients respond to conservative measures, with a surgical consultation reserved for those who have progressive pain, altered sensation, skin ulceration, skin blistering, or reduced capillary refill [44]. The risk of tissue damage is greater with the higher osmolar GBCAs [17]. Overall though, the risk of tissue loss is less than with iodinated contrast used in CT, due to its relative lower osmolarity and also due to the lower volumes of contrast media typically used in cardiovascular MRI compared with CT.

## Nephrogenic Systemic Fibrosis (NSF)

Nephrogenic systemic fibrosis (NSF) is an acquired fibrosing condition characterized by thickening, induration, and tightening of the skin with subcutaneous edema. It may be locally confined to the skin or may have systemic involvement affecting the lungs, skeletal muscle, heart, pericardium, and kidneys [48]. It is a serious condition, which can be fatal. The skin thickening and tethering are associated with increased pigmentation, often beginning in the lower extremities before progressing cranially [49]. Diagnosis can be difficult, requiring a detailed dermatological examination, combined with light microscopy of skin punch biopsy. A combined clinic-pathological diagnostic scoring system has been developed by the NSF registry in New Haven (CT, USA) to aid in the evaluation of suspected cases of NSF [50]. The typical features of NSF are listed in Table 8.2.

**Table 8.2** Clinical features of nephrogenic systemic fibrosis [50]

System	Clinical feature
Skin	Symmetric, bilateral fibrotic indurated papules, plaques, or subcutaneous nodules Subcutaneous edema may give rise to a peau d'orange pattern Commonly involves lower and upper limbs Trunk less frequently affected Head typically spared
Musculoskeletal	Muscle induration and joint contractures can be seen with severe disease
Eyes	Asymptomatic yellowish scleral plaques are common
Viscera	Visceral fibrosis can affect the lungs, diaphragm, myocardium, pericardium, pleura, and dura mater

NSF can occur as a late reaction in patients with severe chronic or acute renal failure after GBCA exposure. The association between this progressive fibrosing condition and GBCA exposure was first described in 2006 [51]. Prior to this, GBCAs had been routinely administered to patients with renal impairment and dialysis patients, patients in whom iodinated contrast is relatively contraindicated. Following the initial reports, the FDA issued a “black box” warning on the use of GBCAs in patients with severe renal impairment [52], followed by a similar warning from the EMA [53]. Clinical manifestations of NSF usually occur within 12 weeks of GBCA administration [50], but some series report delayed onset of symptoms of up to 3 years [54]. This latency period may be even longer in selected cases, with one case report of a 10-year interval between GBCA exposure and NSF presentation [55].

The risk of NSF post GBCA exposure depends on three factors: the patient’s renal function, the type of GBCA used, and the dose administered [56]. Of these, renal function is the most important risk factor. The risk is greatest in patients on renal dialysis, in patients with stage 5 chronic kidney disease (GFR < 30 ml/min) not on dialysis, and in patients with acute kidney injury (AKI). The risk is dependent on the severity of renal dysfunction, regardless of its etiology or duration [54]. One retrospective study found an incidence of NSF of 18% in patients with stage 5 chronic kidney disease (CKD) post gadodiamide administration [57]. In contrast, the risk of NSF is lower in patients with CKD stages 1–4 [57, 58].

The type of GBCA used greatly influences the risk of developing NSF. Almost all of the reported cases of NSF have been reported after exposure to gadodiamide, gadoversetamide, or gadopentetate dimeglumine. A comprehensive review of the 1395 cases of NSF reported up to 2014 found that 76.2% of cases had exposure to gadodiamide, 40.1% to gadopentetate dimeglumine, and 7.3% to gadoversetamide [59]. Both the FDA and EMA classify these three GBCAs as high-risk agents in terms of NSF risk [56]. Gadodiamide has the most amount of reported cases of NSF, with a three- to sevenfold higher risk than other GBCAs in patients with renal impairment [60]. In vulnerable patients, the dose of GBCA administered is a contributing factor in the risk of developing NSF. A retrospective analysis of 300 patients who received gadodiamide found an increased incidence of NSF in patients with renal impairment that received twice the regular dose (0.2 mmol/kg), compared with patients who received a standard dose (0.1 mmol/kg) [61].

The differential NSF risk among the licensed GBCAs is due mainly to differences in their chemical structure. As described in earlier sections, the macrocyclic agents offer better protection of the toxic  $Gd^{3+}$  ions than their linear counterparts. Among the linear agents, the nonionic compounds have the weakest binding between the ligand and the  $Gd^{3+}$  ion, due to the reduced number of binding carboxyl groups. These linear nonionic compounds are the least stable agents and thus have the highest NSF risk.

The exact mechanism by which NSF occurs has not yet been fully elucidated. One theory is that  $Gd^{3+}$  is caused to dissociate from the GBCA compound by the binding of endogenous cations in plasma, such as  $Fe^{3+}$ ,  $Zn^{2+}$ ,  $Cu^{2+}$ , and  $Ca^{2+}$ , to the chelating ligand. This process is called transmetallation. Supporting this theory are several studies demonstrating alterations in serum levels of these endogenous elements following GBCA exposure [62–64]. Zinc is the main cation that displaces  $Gd^{3+}$ , due to its high blood concentrations. The transmetallation process occurs preferably in patients with renal impairment due to the increase in elimination half-life of the GBCA. In patients with normal renal function, this is approximately 90 min and can be prolonged to over 24 h in patients with advanced renal impairment.

Free  $Gd^{3+}$  ions, once released from the chelator through this process, bind to endogenous anions, particularly phosphate ( $PO_4^-$ ). The resulting complexes between gadolinium ions and endogenous anions form insoluble salts, which precipitate and deposit in tissues. These salts are then engulfed by circulation macrophages, which release multiple proinflammatory and profibrotic cytokines. These in turn attract circulating fibrocytes, which begin to synthesize and deposit a fibrotic extracellular matrix [49, 56, 65]. This excess of fibrotic tissue manifests clinically as the dermal and visceral fibrosis that characterizes NSF.

Several different therapies have been trialed for NSF, such as plasmapheresis, phototherapy, and monoclonal antibodies, but no agents have to date proved curative [56]. Restoration of normal renal function is the only strategy which has been proven to halt NSF progression, and cure has been reported in patients post recovery from AKI and following successful renal transplantation [66].

With these limitations in NSF treatment, the emphasis is on prevention. This depends on appropriate GBCA use, namely, in terms of the choice of agent, dose of agent, and patient selection. Patients with CKD 4 and 5, patients on dialysis (hemodialysis and peritoneal dialysis), and patients with AKI have the highest risk for developing NSF. Patients with CKD 3 (eGFR 30–59 ml/min) are at a lower risk, and there are no cases to date of NSF reported in patients with an eGFR >60 ml/min [67]. Almost all confirmed cases of NSF followed exposure to a linear nonionic GBCA.

Once at-risk patients are identified, strategies to prevent NSF include performing MRI without GBCA, performing an alternative imaging modality, and delaying the examination until renal function improves. If performing an MRI with GBCA is deemed essential, then an agent with a low NSF risk (macrocyclic agents) should be used, at the lowest dose possible in order to obtain diagnostic image quality. No cases of NSF were reported in reviews of almost 400 patients on dialysis who received either gadoterate or gadoteridol, both macrocyclic GBCAs [68, 69]. Performing hemodialysis post GBCA exposure in vulnerable patients cannot reverse fibrotic tissue formation, but it can remove the contrast agent [70]. If it is to

be performed, one suggested regimen is to start hemodialysis within 2 h of GBCA exposure and to perform several additional sessions over subsequent consecutive days [71]. There is no current recommendation for patients on peritoneal dialysis.

Since the link between NSF and GBCAs was established in the mid-2000s, the number of reported cases has reduced dramatically with the prudent use of GBCAs in at-risk patients. It has not been completely eliminated, however, and continued vigilance is necessary.

### **Gadolinium Deposition in Patients with Normal Renal Function**

It was widely believed up until the recent few years that GBCAs were completely eliminated from the body in patients with normal renal function. However, there is emerging data demonstrating tissue gadolinium accumulation in patients with normal renal function post GBCA exposure [65]. This deposition had been demonstrated in studies of postmortem neuronal tissue, with the greatest accumulation reported in the dentate nucleus, with lesser amounts detected in the thalamus, dentate, pons, and globus pallidus [72]. The neuronal deposition can be associated with dose-dependent increased SI on non-contrast T1-weighted sequences, most marked in the dentate nucleus in the cerebellum and in the globus pallidus [73]. As described with NSF risk, the rates of brain deposition appear to correlate with the stability of the GBCA used. The agent most associated with neuronal deposition is the linear nonionic GBCA gadodiamide [74]. The more stable macrocyclic agents have, in general, not been associated with significant increases in cerebral T1 SI [75]. The macrocyclic GBCAs, however, do not seem to be completely without risk, with brain deposition reported following exposure to the macrocyclic nonionic agent gadobutrol [73]. This suggests that the risk of brain deposition cannot be solely evaluated based solely on GBCA ligand-structure morphology. The only GBCA which has not yet been associated with either increased cerebral T1 signal or pathological neuronal deposition is the macrocyclic ionic agent gadoterate meglumine [76].

Gadolinium accumulation has also been reported in the bone and skin in patients with normal renal function at the time of GBCA exposure [77, 78]. Darrach et al. found evidence of gadolinium deposition in femoral head bone samples collected at the time of total hip replacement, up to 8 years after GBCA exposure [79]. It is unclear yet whether the accumulated gadolinium represents free or chelated  $Gd^{3+}$ ; however, the greater concentrations of tissue deposition associated with the less stable GBCAs (linear nonionic) suggest the deposition is predominantly free  $Gd^{3+}$ . The known toxic effects of free  $Gd^{3+}$  result from either its ability to compete competitively with  $Ca^{2+}$  or its insolubility at physiologic pH, causing it to precipitate as an insoluble salt causing local macrophage activation, as previously described.

The clinical significance and long-term effects, if any, of the tissue gadolinium accumulation observed in patients with normal renal function are not yet clear. All GBCAs probably deposit in vivo to some degree, but at present it is only the weaker linear chelates that have been definitively linked to a meaningful disease in NSF. It is likely that the amount of gadolinium tissue deposition strongly influences the development of a definite clinical entity. No definitive clinical syndrome resulting from this gadolinium deposition has yet been isolated, but it is under investigation by the FDA [80]. Its ultimate significance is yet to be determined.

### **GBCAs and Sickle Cell Disease**

The administration of GBCAs to patients with sickle cell disease has previously been an issue of controversy. In vitro studies have demonstrated that deoxygenated red blood cells align perpendicular to the magnetic field [81]. It has thus been suggested that the increased magnetic moments associated with the administration of a paramagnetic contrast agent may increase the proportional perpendicular alignment, precipitating a vaso-occlusive crisis. Despite this, there have been no documented cases of vaso-occlusive or hemolytic complications related to GBCAs to date [82]. The use of GBCAs in cardiovascular MRI for patients with sickle cell disease does not appear to be associated with increased frequency of adverse events.

### **GBCAs and Pregnancy**

Pregnant women and breastfeeding mothers are a special population group with regard to GBCA exposure. There is little data on GBCA administration in pregnancy and uncertainty as to whether GBCAs can enter the fetal circulation via the placenta. Given the recent reports of gadolinium tissue deposition, the advice in current guidelines against administering GBCAs in pregnancy in the absence of a very strong clinical indication are prudent. When imaging lactating mothers, one of the more stable macrocyclic agents should be used, and breastfeeding should be stopped for 24 h post contrast administration to limit possible infant exposure. To date, there have been no reported cases of adverse events occurring in infants that are breastfeeding after maternal GBCA exposure, but a cautious approach should be taken given the infant's immature renal system.

### **GBCAs and the Environment**

In the past number of years, there have been increasing reports of the detection of anthropogenic (pollutant) rare-earth metals

in surface water. Chief among them has been the detection of anthropogenic gadolinium in surface and drinking water [83–86]. The cause of this is felt to be largely due to the use of GBCAs in medical imaging, and some of the highest concentrations are to be found near to medical facilities [83]. The concentrations that have been found in the ecosystem are well below those that could be harmful to the aquatic ecosystem. To date, there have been no adverse outcomes reported from the presence of trace anthropogenic gadolinium in drinking water, but this is under continued surveillance by the environmental regulatory agencies.

## Non-gadolinium-Based Cardiovascular MR Contrast Agents

### Iron Oxide Nanoparticles

Iron oxide nanoparticles (ION) have been investigated over the last two decades as potential alternative MRI contrast agents. Below a certain particle size, they exhibit superparamagnetic properties, strongly reducing T1, T2, and T2\* relaxation times. They differ from paramagnetic agents in that they only exhibit magnetization when in the presence of an external magnetic field. Structurally they consist of a magnetic iron oxide core, covered in a nonmagnetic polymer coating. The coating is crucial for making the agent soluble and usually consists of the polysaccharide dextran or a derivative. After intravenous administration, they disperse in the blood pool. They do not undergo renal excretion; rather, they are taken up by monocytes/macrophages and are incorporated in the reticuloendothelial system [87]. They can be classified according to their size into superparamagnetic iron oxide particles (SPIO) measuring 50–250 nm and ultra-small SPIO (USPIO) measuring 20–50 nm. USPIOs cause a strong reduction in T1, T2, and T2\* relaxation times. This results in significant signal loss on T2-weighted images, but it does also significantly shorten T1 relaxation, allowing its use as a positive contrast agent with T1-weighted imaging.

### Ferumoxytol

Ferumoxytol is an USPIO agent that has been under investigation as an MR contrast agent for over a decade [88]. It has been approved by the FDA as a therapeutic preparation for the treatment of iron-deficient anemia in patients with chronic kidney disease [89]. Its use as an MR contrast agent is currently off-label. Given the risks outlined of using GBCAs in patients with severe renal dysfunction, ferumoxytol has emerged as an attractive alternative.

Due to its relatively small size (approximately 30 nm), carbohydrate coating and neutral charge ferumoxytol have a prolonged intravascular time of 12–15 h, allowing for a long

vascular imaging window [87, 90]. As a USPIO agent, it undergoes phagocytosis by macrophages after a delay, concentrating it in areas of increased inflammation. This unique property allows for the identification of pathological areas of inflammation [91].

Intravenous iron is associated with a risk of anaphylaxis and hypotension. Ferumoxytol was specifically designed to minimize the risk of a severe adverse reaction; nevertheless, serious adverse reactions do occur. The reported rates of anaphylaxis with its therapeutic use ranges from 0.02% to 1.3% [92]. In 2015, the FDA issued a black box warning on the use of ferumoxytol, with 79 cases of anaphylaxis reported after approximately 1.2 million therapeutic doses [93]. The mechanism of this reaction is felt to be due to bioactive-free iron causing mast cell degranulation [94]. The overall risk of serious adverse events appears similar to that of iodinated contrast media, and higher than GBCAs, although the latter comparison is mitigated somewhat by its superior safety profile in patients with renal impairment.

Typical imaging doses of ferumoxytol are usually 1.5–4 mg/kg, diluted with normal saline at a ratio of 1 part ferumoxytol to 4 parts saline [88, 90, 92]. This is significantly less than the therapeutic dose for treating anemia of 1020 mg, approximately 14.6 mg/kg for a 70 kg adult. For vascular MRI, injection rates of 2 ml/s are commonly used, followed by a saline chaser [90]. MR image SI may be altered by ferumoxytol for days to months after administration, be it for therapeutic or diagnostic purposes. This allows for the use of slower, high-resolution 3D MRA techniques [95]. High injection rates have been associated with signal loss artifact on T1-weighted images during arterial phase imaging which can mimic thrombus, likely due to T2\*-shortening effects of concentrated ferumoxytol [96].

Ferumoxytol has a number of potential applications in cardiovascular imaging. It has been successfully used in aortic and peripheral vascular imaging, with potential applications in coronary artery MRA and cardiac MRI [90, 97]. Studies in patients with myocardial infarction suggest that ferumoxytol may be useful in estimating the size of the infarct up to 96 h after administration due to its increase macrophage uptake in infarcted myocardium, manifesting as signal loss on T2-weighted imaging [98, 99].

### Other Iron Oxide Agents

Aside from ferumoxytol, a number of other USPIOs have been investigated as potential MR contrast agents. Ferumoxtran-10 is an USPIO agent with similar properties to ferumoxytol with a dextran polymer coating [87]. It was extensively investigated as a potential cardiovascular MR contrast agent in clinical studies but was discontinued in 2010. The carboxydextran-covered agent ferucarbotran (Resovist), a SPIO agent, was previously approved for use in



liver imaging and was investigated as a potential CMR contrast agent before it was discontinued from clinical use in 2009 [87]. Recently, there has been interest in another group of IONs that are even smaller than USPIOs, called very small SPIOs (VSPIO) with a size <20 nm, although these agents are still at the experimental phase [100]. The ability of USPIOs enhanced MRI to detect inflammatory processes associated with a range of cardiovascular pathology is an exciting prospect, with a number of potential clinical applications.

## Manganese-Based Contrast Agents

Manganese (Mn<sup>2+</sup>) is an essential element of human diet and a paramagnetic lanthanide metal. It has five unpaired electrons, which accounts for its powerful paramagnetic properties, shortening both T<sub>1</sub> and T<sub>2</sub> relaxation times considerably. It is toxic in its free form and is thus chelated onto a ligand for clinical use. Mangafodipir trisodium (Telescan, GE healthcare, Milwaukee, WI) is the commercially available manganese-based contrast agent, consisting of the manganese ion chelated to dipyrindol diphosphate. T<sub>1</sub>-shortening effects predominate at lower concentrations, with T<sub>2</sub>-shortening effects predominating at higher concentrations. It is taken up by hepatocytes and predominantly excreted via the biliary system, a feature which is taken advantage of in its principal application in hepatic MRI [101]. Mangafodipir trisodium was investigated as a potential MR contrast agent for first-pass myocardial perfusion imaging, but has not been widely adopted in clinical practice.

Other manganese-based contrast agents are currently under investigation as potential cardiovascular MR contrast agents. Manganese chloride is one such agent, with potential as an intracellular contrast agent [102]. Free manganese ions act as calcium analogues, are taken up into myocardial cells via voltage-gated calcium channels, and are then retained in myocyte mitochondria. This intracellular uptake potentially allows for the detection of infarcted myocardium with accuracy [102]. There are concerns about the use of manganese as an intracellular contrast agent at high doses due to the possibility of inducing acute heart failure. An initial study on humans has demonstrated safety of magnesium chloride as a cardiac MR contrast agent when used at a small dose [102]. Further clinical studies, however, are required if it is to become a clinically useful contrast agent for cardiovascular imaging.

---

## Clinical Applications

### Magnetic Resonance Angiography (MRA)

Contrast-enhanced magnetic resonance angiography (CE-MRA) techniques provide excellent angiographic

images without radiation. Modern MRA techniques, such as centric k-space filling and parallel imaging, allow for arterial phase imaging without venous contamination with excellent SNR and CNR. In terms of contrast agents used in MRA, GBCAs predominate, with recent interest in the use of ferumoxylol in selected patients. GBCAs with high relaxivity that remain within the blood pool are the most attractive from an image quality point of view. However, safety considerations, such as NSF risk and brain deposition, must also be taken into account when choosing a GBCA for MRA. The linear ionic GBCA gadobenate dimeglumine is still the most commonly used contrast agent in CE-MRA. Although it is not an intravascular agent, it does have a higher degree of protein binding than the majority of the other GBCAs and has a relatively higher relaxivity. Gadobenate dimeglumine provides diagnostic MRA quality compared with the traditional vascular imaging gold standard, invasive digital subtraction angiography (DSA) [103].

The approval of the first predominantly intravascular GBCA, the linear ionic agent gadofosveset trisodium was much heralded due to its high relaxivity and high protein binding. Its added diagnostic benefit above that of the ECF GBCAs, however, has not proved to be universally accepted. Since its initial approval by the EMA in 2007, it has since been withdrawn from the EU for commercial reasons. Several direct comparisons with gadobenate dimeglumine have not revealed a significant improvement in arterial phase image quality [104–106]. Gadofosveset trisodium does offer an advantage over the extracellular GBCAs in intravascular SI in equilibrium phase imaging performed more than 15 min postinjection [107].

Concerns over the safety of GBCAs are important when choosing an agent for MRA. Both gadobenate dimeglumine and gadofosveset trisodium are linear ionic agents, placing them in the intermediate risk category for the development of NSF in susceptible patients. The recent discovery of cerebral gadolinium deposition in patients with normal renal function is also of concern, although the clinical significance of this phenomenon is yet to be determined. The currently available GBCA with the most favorable risk profile in terms of NSF and cerebral deposition is the macrocyclic ionic agent gadoterate meglumine. This agent has inferior protein binding and relaxivity compared with some of the other GBCAs, but this is somewhat offset by its safety profile. Its macrocyclic, ionic structure renders it a highly stable GBCA. There have to date been no reported cases of NSF with this agent, even in patient with severe renal dysfunction [108, 109], and it is also the only GBCA in which cerebral deposition has not been demonstrated [76]. In patients whom GBCA administration is not desirable, the USPIO agent ferumoxylol has recently emerged as a viable alternative, providing diagnostic quality MRA images, although concerns do exist about its risk of hypersensitivity reaction.

## Cardiac Magnetic Resonance (CMR)

One of the major advantages of CMR as an imaging modality is its ability to distinguish damaged from normal myocardium. The use of MR contrast is crucial to this. As described before, extracellular GBCAs rapidly dissociate into the extracellular space after intravenous administration, before slowly washing out again. The increased extracellular space found in areas of infarcted or edematous myocardium results in accumulation of ECF GBCA, manifesting as increased SI on T1-weighted imaging relative to normal myocardium. This helps differentiate normal from damaged myocardium and is the basis behind the use of late gadolinium enhancement (LGE) imaging, performed 10–20 min after GBCA administration. LGE imaging is a fast, robust, reproducible method of determining myocardial viability in patients with reduced left ventricular function and can predict the likelihood of recovery in contractile function post revascularization [110, 111]. To achieve good LGE imaging, it is preferable to use a GBCA that is not highly protein-bound, allowing it to freely dissociate into the extracellular space. This is the converse of the features desirable in a CE-MRA agent. To assess for myocardial viability, the ideal contrast agent would be one that is taken up by myocardial myocytes, but there are no such commercially available MR contrast agents. The linear ionic GBCA gadopentete dimeglumine was traditionally the most commonly used agent, usually at a dose of 0.15–0.2 mmol/kg. There are safety concerns about this agent, and the other linear GBCAs, primarily due to the risk of NSF. As a result, many institutions have switched to using macrocyclic agents GBCAs in CMR, such as gadobutrol and gadoterate meglumine at a dose of 0.1–0.15 mmol/kg, without a significant deterioration in diagnostic image quality [112].

Aside from LGE imaging, the assessment of myocardial perfusion in patients with suspected coronary artery disease is the other major reason to use contrast in CMR. In myocardial perfusion imaging (MPI), the increase in myocardial SI during the first pass of a GBCA bolus through the myocardial microcirculation correlates with coronary blood flow, with significant CAD manifesting as segmental areas of hypoperfusion in a typical coronary arterial distribution [113, 114]. This can be performed both at rest and after administration of a pharmacological vasodilator stress agent such as adenosine or regadenoson. Quantitative myocardial perfusion techniques are now available, allowing more accurate assessment of myocardial blood flow [115].

## Conclusion

The use of contrast in clinical cardiovascular MRI is crucial in improving the ability to make accurate diagnoses. Advances in MR technology bring exciting new possibilities for the use of contrast media in cardiovascular MR,

but continued vigilance is required to ensure the highest standards of patient safety.

## References

1. Damadian R, Goldsmith M, Minkoff L. NMR in cancer: XVI. FONAR image of the live human body. *Physiol Chem Phys*. 1977;9(1):97–100, 108.
2. Shokrollahi H. Contrast agents for MRI. *Mater Sci Eng C Mater Biol Appl*. 2013;33(8):4485–97.
3. Bottrill M, Kwok L, Long NJ. Lanthanides in magnetic resonance imaging. *Chem Soc Rev*. 2006;35(6):557–71.
4. Brady TJ, Goldman MR, Pykett IL, Buonanno FS, Kistler JP, Newhouse JH, et al. Proton nuclear magnetic resonance imaging of regionally ischemic canine hearts: effect of paramagnetic proton signal enhancement. *Radiology*. 1982;44(2):343–7.
5. Young IR, Clarke GJ, Bailes DR, Pennock JM, Doyle FH, Bydder GM. Enhancement of relaxation rate with paramagnetic contrast agents in NMR imaging. *J Comput Tomogr*. 1981;5(6):543–7.
6. Weinmann HJ, Brasch RC, Press WR, Wesbey GE. Characteristics of gadolinium-DTPA complex: a potential NMR contrast agent. *Am J Roentgenol*. 1984;142(3):619–24.
7. Laniado M, Weinmann HJ, Schörner W, Felix R, Speck U. First use of GdDTPA/dimeglumine in man. *Physiol Chem Phys Med NMR*. 1984;16(2):157–65.
8. Lohrke J, Frenzel T, Endrikat J, Alves FC, Grist TM, Law M, et al. 25 years of contrast-enhanced MRI: developments, current challenges and future perspectives. *Adv Ther*. 2016;33(1):1–28.
9. Sherry AD, Caravan P, Lenkinski RE. Primer on gadolinium chemistry. *J Magn Reson Imaging*. 2009;30(6):1240–8.
10. Port M, Idée J-M, Medina C, Robic C, Sabatou M, Corot C. Efficiency, thermodynamic and kinetic stability of marketed gadolinium chelates and their possible clinical consequences: a critical review. *Biometals*. 2008;21(4):469–90.
11. Oksendal AN, Hals PA. Biodistribution and toxicity of MR imaging contrast media. *J Magn Reson Imaging*. 1993;3(1):157–65.
12. Frenzel T, Lengsfeld P, Schirmer H, Hütter J, Weinmann H-J. Stability of gadolinium-based magnetic resonance imaging contrast agents in human serum at 37 degrees C. *Investig Radiol*. 2008;43(12):817–28.
13. Hao D, Ai T, Goerner F, Hu X, Runge VM, Tweedle M. MRI contrast agents: basic chemistry and safety. *J Magn Reson Imaging*. 2012;36(5):1060–71.
14. Laurent S, Elst LV, Muller RN. Comparative study of the physicochemical properties of six clinical low molecular weight gadolinium contrast agents. *Contrast Media Mol Imaging*. 2006;1(3):128–37.
15. Tweedle MF, Hagan JJ, Kumar K, Mantha S, Chang CA. Reaction of gadolinium chelates with endogenously available ions. *Magn Reson Imaging*. 1991;9(3):409–15.
16. Schmitt-Willich H. Stability of linear and macrocyclic gadolinium based contrast agents. *Br J Radiol*. 2007;80(955):581–2.
17. Runge VM, Dickey KM, Williams NM, Peng X. Local tissue toxicity in response to extravascular extravasation of magnetic resonance contrast media. *Investig Radiol*. 2002;37(7):393–8.
18. Rose TA, Choi JW. Intravenous imaging contrast media complications: the basics that every clinician needs to know. *Am J Med*. 2015;128(9):943–9.
19. Aime S, Caravan P. Biodistribution of gadolinium-based contrast agents, including gadolinium deposition. *J Magn Reson Imaging*. 2009;30(6):1259–67.
20. Seale MK, Catalano OA, Saini S, Hahn PF, Sahani DV. Hepatobiliary-specific MR contrast agents: role in imaging the liver and biliary tree. *Radiographics*. 2009;29(6):1725–48.

21. Tombach B, Bremer C, Reimer P, Schaefer RM, Ebert W, Geens V, et al. Pharmacokinetics of 1M gadobutrol in patients with chronic renal failure. *Investig Radiol.* 2000;35(1):35–40.
22. Schuhmann-Giampieri G, Krestin G. Pharmacokinetics of Gd-DTPA in patients with chronic renal failure. *Investig Radiol.* 1991;26(11):975–9.
23. de Haën C, Cabrini M, Akhanna L, Ratti D, Calabi L, Gozzini L. Gadobenate dimeglumine 0.5 M solution for injection (MultiHance) pharmaceutical formulation and physicochemical properties of a new magnetic resonance imaging contrast medium. *J Comput Assist Tomogr.* 1999;23(Suppl 1):S161–8.
24. Huppertz A, Balzer T, Blakeborough A, Breuer J, Giovagnoni A, Heinz-Peer G, et al. Improved detection of focal liver lesions at MR imaging: multicenter comparison of gadoxetic acid-enhanced MR images with intraoperative findings. *Radiology.* 2004;230(1):266–75.
25. Caravan P, Cloutier NJ, Greenfield MT, McDermid SA, Dunham SU, Bulte JWM, et al. The interaction of MS-325 with human serum albumin and its effect on proton relaxation rates. *J Am Chem Soc.* 2002;124(12):3152–62.
26. Lauffer RB, Parmelee DJ, Dunham SU, Ouellet HS, Dolan RP, Witte S, et al. MS-325: albumin-targeted contrast agent for MR angiography. *Radiology.* 1998;2:529–38.
27. Grist TM, Korosec FR, Peters DC, Witte S, Walovitch RC, Dolan RP, et al. Steady-state and dynamic MR angiography with MS-325: initial experience in humans. *Radiology.* 1998;207(2):539–44.
28. Parmelee DJ, Walovitch RC, Ouellet HS, Lauffer RB. Preclinical evaluation of the pharmacokinetics, biodistribution, and elimination of MS-325, a blood pool agent for magnetic resonance imaging. *Investig Radiol.* 1997;32(12):741–7.
29. Sabach AS, Bruno M, Kim D, Mulholland T, Lee L, Kaura S, et al. Gadofosveset trisodium: abdominal and peripheral vascular applications. *Am J Roentgenol.* 2013;200(6):1378–86.
30. Spanakis M, Marias K. In silico evaluation of gadofosveset pharmacokinetics in different population groups using the Simcyp simulator platform. In *Silico Pharmacol.* 2014 Dec;2(1):1–9.
31. Caravan P, Comuzzi C, Crooks W, McMurry TJ, Choppin GR, Woulfe SR. Thermodynamic stability and kinetic inertness of MS-325, a new blood pool agent for magnetic resonance imaging. *Inorg Chem.* 2001;40(9):2170–6.
32. Wendland MF, Saeed M, Masui T, Derugin N, Higgins CB. First pass of an MR susceptibility contrast agent through normal and ischemic heart: gradient-recalled echo-planar imaging. *J Magn Reson Imaging.* 1993;3(5):755–60.
33. Sakuma H, O’Sullivan M, Lucas J, Wendland MF, Saeed M, Dulce MC, et al. Effect of magnetic susceptibility contrast medium on myocardial signal intensity with fast gradient-recalled echo and spin-echo MR imaging: initial experience in humans. *Radiology.* 1994;190(1):161–6.
34. Dumas S, Jacques V, Sun W-C, Troughton JS, Welch JT, Chasse JM, et al. High relaxivity magnetic resonance imaging contrast agents. Part 1. Impact of single donor atom substitution on relaxivity of serum albumin-bound gadolinium complexes. *Investig Radiol.* 2010;45(10):600–12.
35. Varga-Szemes A, Kiss P, Rab A, Suranyi P, Lenkey Z, Simor T, et al. In vitro Longitudinal Relaxivity Profile of Gd(ABE-DTTA), an investigational magnetic resonance imaging contrast agent. *Radiographics.* 2016;11(2):e0149260.
36. Brockow K, Ring J. Anaphylaxis to radiographic contrast media. *Curr Opin Allergy Clin Immunol.* 2011;11(4):326–31.
37. American College of Radiology (ACR). ACR Committee on Drugs and Contrast Media. ACR Manual on Contrast Media Version 10.1 2015. Available from: <http://www.acr.org/~media/37D84428BF1D4E1B9A3A2918DA9E27A3.pdf>. Last accessed 26 Feb 2017.
38. Prince MR, Zhang H, Zou Z, Staron RB, Brill PW. Incidence of immediate gadolinium contrast media reactions. *Am J Roentgenol.* 2011;196(2):W138–43.
39. Dillman JR, Ellis JH, Cohan RH, Strouse PJ, Jan SC. Frequency and severity of acute allergic-like reactions to gadolinium-containing i.v. contrast media in children and adults. *Am J Roentgenol.* 2007;189(6):1533–8.
40. Aran S, Shaqdan KW, Abujudeh HH. Adverse allergic reactions to linear ionic gadolinium-based contrast agents: experience with 194, 400 injections. *Clin Radiol.* 2015;70(5):466–75.
41. Bruder O, Schneider S, Pilz G, van Rossum AC, Schwitter J, Nothnagel D, et al. Update on acute adverse reactions to gadolinium based contrast agents in cardiovascular MR. large multinational and multi-ethnic population experience with 37788 patients from the EuroCMR registry. *J Cardiovasc Magn Reson.* 2015;17:58.
42. Palkowitsch PK, Bostelmann S, Lengsfeld P. Safety and tolerability of iopromide intravascular use: a pooled analysis of three non-interventional studies in 132,012 patients. *Acta Radiol.* 2014;55(6):707–14.
43. Raisch DW, Garg V, Arabyat R, Shen X, Edwards BJ, Miller FH, et al. Anaphylaxis associated with gadolinium-based contrast agents: data from the Food and Drug Administration’s adverse event reporting system and review of case reports in the literature. *Expert Opin Drug Saf.* 2014;13(1):15–23.
44. Beckett KR, Moriarity AK, Langer JM. Safe use of contrast media: what the radiologist needs to know. *Radiographics.* 2015;35(6):1738–50.
45. Jung J-W, Kang H-R, Kim M-H, Lee W, Min K-U, Han M-H, et al. Immediate hypersensitivity reaction to gadolinium-based MR contrast media. *Radiology.* 2012;264(2):414–22.
46. The Royal College of Radiologists. Standards for intravascular contrast agent administration to adult patients. 3rd ed. London: Royal College of Radiologists; 2015. p. 1–22. Available from: [https://www.rcr.ac.uk/sites/default/files/Intravasc\\_contrast\\_web.pdf](https://www.rcr.ac.uk/sites/default/files/Intravasc_contrast_web.pdf). Last accessed 26 Feb 2017.
47. Jingu A, Fukuda J, Taketomi-Takahashi A, Tsushima Y. Breakthrough reactions of iodinated and gadolinium contrast media after oral steroid premedication protocol. *BMC Med Imaging.* 2014;14:34.
48. Kribben A, Witzke O, Hillen U, Barkhausen J, Daul AE, Erbel R. Nephrogenic systemic fibrosis: pathogenesis, diagnosis, and therapy. *J Am Coll Cardiol.* 2009;53(18):1621–8.
49. Thomsen HS. Nephrogenic systemic fibrosis: a serious adverse reaction to gadolinium – 1997–2006–2016. Part 1. *Acta Radiol.* 2016;57(5):515–20.
50. Girardi M, Kay J, Elston DM, Leboit PE, Abu-Alfa A, Cowper SE. Nephrogenic systemic fibrosis: clinicopathological definition and workup recommendations. *J Am Acad Dermatol.* 2011;65(6):1095–7.
51. Grobner T. Gadolinium – a specific trigger for the development of nephrogenic fibrosing dermopathy and nephrogenic systemic fibrosis? *Nephrol Dial Transplant.* 2006;21(4):1104–8.
52. U.S. Food and Drug Administration. A Public Health Advisory. Gadolinium-containing contrast agents for magnetic resonance imaging (MRI). 2006. Available from: <http://www.fda.gov/Drugs/DrugSafety/PostmarketDrugSafetyInformationforPatientsandProviders/DrugSafetyInformationforHealthcareProfessionals/PublicHealthAdvisories/ucm053112.htm>. Last accessed 26 Feb 2017.
53. European Medicines Agency. Vasovist and nephrogenic systemic fibrosis (NSF). 2009. Available from: [http://www.ema.europa.eu/ema/index.jsp?curl=pages/news\\_and\\_events/news/2009/11/news\\_detail\\_000418.jsp&mid=WC0b01ac058004d5c1](http://www.ema.europa.eu/ema/index.jsp?curl=pages/news_and_events/news/2009/11/news_detail_000418.jsp&mid=WC0b01ac058004d5c1). Last accessed 26 Feb 2017.
54. Abujudeh HH, Kaewlai R, Kagan A, Chibnik LB, Nazarian RM, High WA, et al. Nephrogenic systemic fibrosis after gadopentetate



- dimeglumine exposure: case series of 36 patients. *Radiology*. 2009;253(1):81–9.
55. Larson KN, Gagnon AL, Darling MD, Patterson JW, Cropley TG. Nephrogenic systemic fibrosis manifesting a decade after exposure to gadolinium. *JAMA Dermatol*. 2015;151(10):1117–20.
  56. Daftari Besheli L, Aran S, Shaqdan K, Kay J, Abujudeh H. Current status of nephrogenic systemic fibrosis. *Clin Radiol*. 2014;69(7):661–8.
  57. Rydahl C, Thomsen HS, Marckmann P. High prevalence of nephrogenic systemic fibrosis in chronic renal failure patients exposed to gadodiamide, a gadolinium-containing magnetic resonance contrast agent. *Investig Radiol*. 2008;43(2):141–4.
  58. Shabana WM, Cohan RH, Ellis JH, Hussain HK, Francis IR, Su LD, et al. Nephrogenic systemic fibrosis: a report of 29 cases. *Am J Roentgenol*. 2008 Mar;190(3):736–41.
  59. Edwards BJ, Laumann AE, Nardone B, Miller FH, Restaino J, Raisch DW, et al. Advancing pharmacovigilance through academic-legal collaboration: the case of gadolinium-based contrast agents and nephrogenic systemic fibrosis—a research on adverse drug events and reports (RADAR) report. *Br J Radiol*. 2014;87(1042):20140307.
  60. Thomsen HS, Marckmann P. Extracellular Gd-CA: differences in prevalence of NSF. *Eur J Radiol*. 2008;66(2):180–3.
  61. Broome DR, Girguis MS, Baron PW, Cottrell AC, Kjellin I, Kirk GA. Gadodiamide-associated nephrogenic systemic fibrosis: why radiologists should be concerned. *Am J Roentgenol*. 2007;188(2):586–92.
  62. Swaminathan S, Horn TD, Pellowski D, Abul-Ezz S, Bornhorst JA, Viswamitra S, et al. Nephrogenic systemic fibrosis, gadolinium, and iron mobilization. *N Engl J Med*. 2007;357(7):720–2.
  63. Kimura J, Ishiguchi T, Matsuda J, Ohno R, Nakamura A, Kamei S, et al. Human comparative study of zinc and copper excretion via urine after administration of magnetic resonance imaging contrast agents. *Radiat Med*. 2005;23(5):322–6.
  64. High WA, Ayers RA, Chandler J, Zito G, Cowper SE. Gadolinium is detectable within the tissue of patients with nephrogenic systemic fibrosis. *J Am Acad Dermatol*. 2007;56(1):21–6.
  65. Rogosnitzky M, Branch S. Gadolinium-based contrast agent toxicity: a review of known and proposed mechanisms. *Biometals*. 2016;29(3):365–76.
  66. Cuffy MC, Singh M, Formica R, Simmons E, Abu Alfa AK, Carlson K, et al. Renal transplantation for nephrogenic systemic fibrosis: a case report and review of the literature. *Nephrol Dial Transplant*. 2011;26(3):1099–101.
  67. Thomsen HS. Nephrogenic systemic fibrosis: a serious adverse reaction to gadolinium – 1997–2006–2016. Part 2. *Acta Radiol*. 2016;57(6):643–8.
  68. Reilly RF. Risk for nephrogenic systemic fibrosis with gadoteridol (ProHance) in patients who are on long-term hemodialysis. *Am Heart J*. 2008;3(3):747–51.
  69. Amet S, Launay-Vacher V, Clément O, Frances C, Tricotel A, Stengel B, et al. Incidence of nephrogenic systemic fibrosis in patients undergoing dialysis after contrast-enhanced magnetic resonance imaging with gadolinium-based contrast agents: the prospective Fibrose Néphrogénique Systémique study. *Investig Radiol*. 2014;49(2):109–15.
  70. Khawaja AZ, Cassidy DB, Shakarchi AI, McGrogan DG, Inston NG, Jones RG. Revisiting the risks of MRI with gadolinium based contrast agents—review of literature and guidelines. *Insights Imaging*. 2015;6(5):553–8.
  71. European Society of Urogenital Radiology (ESUR). ESUR Contrast Media Safety Committee. ESUR Guidelines on Contrast Media 9.0. 2014. Available from: <http://www.esur.org/esur-guidelines/>. Last accessed 26 Feb 2017.
  72. McDonald RJ, McDonald JS, Kallmes DF, Jentoft ME, Murray DL, Thielen KR, et al. Intracranial gadolinium deposition after contrast-enhanced MR imaging. *Radiology*. 2015;275(3):772–82.
  73. Stojanov DA, Aracki-Trenkic A, Vojinovic S, Benedeto-Stojanov D, Ljubisavljevic S. Increasing signal intensity within the dentate nucleus and globus pallidus on unenhanced T1W magnetic resonance images in patients with relapsing-remitting multiple sclerosis: correlation with cumulative dose of a macrocyclic gadolinium-based contrast agent, gadobutrol. *Eur Radiol*. 2016;26(3):807–15.
  74. Ramalho J, Semelka RC, Ramalho M, Nunes RH, AIObaidey M, Castillo M. Gadolinium-based contrast agent accumulation and toxicity: an update. *Am J Neuroradiol*. 2016;37(7):1192–8.
  75. Kanda T, Osawa M, Oba H, Toyoda K, Kotoku J, Haruyama T, et al. High signal intensity in dentate nucleus on unenhanced T1-weighted MR images: association with linear versus macrocyclic gadolinium chelate administration. *Radiology*. 2015;275(3):803–9.
  76. Robert P, Lehericy S, Grand S, Violas X, Fretellier N, Idée J-M, et al. T1-weighted Hypersignal in the deep cerebellar nuclei after repeated administrations of gadolinium-based contrast agents in healthy rats: difference between linear and macrocyclic agents. *Investig Radiol*. 2015;50(8):473–80.
  77. Murata N, Gonzalez-Cuyar LF, Murata K, Fligner C, Dills R, Hippe D, et al. Macrocyclic and other non-group 1 gadolinium contrast agents deposit low levels of gadolinium in brain and bone tissue: preliminary results from 9 patients with normal renal function. *Investig Radiol*. 2016;51(7):447–53.
  78. Roberts DR, Lindhorst SM, Welsh CT, Maravilla KR, Herring MN, Braun KA, et al. High levels of gadolinium deposition in the skin of a patient with normal renal function. *Investig Radiol*. 2016;51(5):280–9.
  79. Darrach TH, Prutsman-Pfeiffer JJ, Poreda RJ, Ellen Campbell M, Hauschka PV, Hannigan RE. Incorporation of excess gadolinium into human bone from medical contrast agents. *Metallomics*. 2009;1(6):479–88.
  80. Food and Drug Administration (FDA). FDA Drug Safety Communication (2015) FDA evaluating the risk of brain deposits with repeated use of gadolinium-based contrast agents for magnetic resonance imaging (MRI). Available from: <http://www.fda.gov/Drugs/DrugSafety/ucm455386.htm>. Last accessed 26 Feb 2017.
  81. Brody AS, Sorette MP, Gooding CA, Listerud J, Clark MR, Mentzer WC, et al. AUR memorial Award. Induced alignment of flowing sickle erythrocytes in a magnetic field. A preliminary report. *Investig Radiol*. 1985;20(6):560–6.
  82. Dillman JR, Ellis JH, Cohan RH, Caoili EM, Hussain HK, Campbell AD, et al. Safety of gadolinium-based contrast material in sickle cell disease. *J Magn Reson Imaging*. 2011;34(4):917–20.
  83. Hatje V, Bruland KW, Flegel AR. Increases in anthropogenic gadolinium anomalies and rare earth element concentrations in San Francisco Bay over a 20 year record. *Environ Sci Technol*. 2016;50(8):4159–68.
  84. Rabiet M, Brissaud F, Seidel JL, Pistre S, Elbaz-Poulichet F. Positive gadolinium anomalies in wastewater treatment plant effluents and aquatic environment in the Hérault watershed (South France). *Chemosphere*. 2009;75(8):1057–64.
  85. Kulaksız S, Bau M. Rare earth elements in the Rhine River, Germany: first case of anthropogenic lanthanum as a dissolved microcontaminant in the hydrosphere. *Environ Int*. 2011;37(5):973–9.
  86. Telgmann L, Wehe CA, Birka M, Künnemeyer J, Nowak S, Sperling M, et al. Speciation and isotope dilution analysis of gadolinium-based contrast agents in wastewater. *Environ Sci Technol*. 2012;46(21):11929–36.
  87. Bietenbeck M, Florian A, Sechtem U, Yilmaz A. The diagnostic value of iron oxide nanoparticles for imaging of myocardial inflammation – quo vadis? *J Cardiovasc Magn Reson*. 2015;17:54.



88. Prince MR, Zhang HL, Chabra SG, Jacobs P, Wang Y. A pilot investigation of new superparamagnetic iron oxide (ferumoxytol) as a contrast agent for cardiovascular MRI. *J Xray Sci Technol*. 2003;11(4):231–40.
89. Lu M, Cohen MH, Rieves D, Pazdur R. FDA report: Ferumoxytol for intravenous iron therapy in adult patients with chronic kidney disease. *Am J Hematol*. 2010;85(5):315–9.
90. Hope MD, Hope TA, Zhu C, Faraji F, Haraldsson H, Ordovas KG, et al. Vascular imaging with Ferumoxytol as a contrast agent. *Am J Roentgenol*. 2015;205(3):W366–73.
91. Gkagkanasiou M, Ploussi A, Gazouli M, Efstathopoulos EP. USPIO-enhanced MRI neuroimaging: a review. *J Neuroimaging*. 2016;26(2):161–8.
92. Vasawala SS, Nguyen K-L, Hope MD, Bridges MD, Hope TA, Reeder SB, et al. Safety and technique of ferumoxytol administration for MRI. *Magn Reson Med*. 2016;75(5):2107–11.
93. Food and Drug Administration (FDA). FDA Drug Safety Communication: FDA strengthens warnings and changes prescribing instructions to decrease the risk of serious allergic reactions with anemia drug Feraheme (ferumoxytol) 2015. Available from: <http://www.fda.gov/Drugs/DrugSafety/ucm440138.htm>. Last accessed 26 Feb 2017.
94. Bircher AJ, Auerbach M. Hypersensitivity from intravenous iron products. *Immunol Allergy Clin North Am*. 2014;34(3):707–23.
95. Mukundan S, Steigler ML, Hsiao L-L, Malek SK, Tullius SG, Chin MS, et al. Ferumoxytol-enhanced magnetic resonance imaging in late-stage CKD. *Am J Kidney Dis*. 2016;67(6):984–8.
96. Fananapazir G, Marin D, Suhocki PV, Kim CY, Bashir MR. Vascular artifact mimicking thrombosis on MR imaging using ferumoxytol as a contrast agent in abdominal vascular assessment. *J Vasc Interv Radiol*. 2014;25(6):969–76.
97. Hanneman K, Kino A, Cheng JY, Alley MT, Vasawala SS. Assessment of the precision and reproducibility of ventricular volume, function, and mass measurements with ferumoxytol-enhanced 4D flow MRI. *J Magn Reson Imaging*. 2016;44(2):383–92.
98. Yilmaz A, Dengler MA, van der Kuip H, Yildiz H, Rösch S, Klumpp S, et al. Imaging of myocardial infarction using ultrasmall superparamagnetic iron oxide nanoparticles: a human study using a multi-parametric cardiovascular magnetic resonance imaging approach. *Eur Heart J*. 2013;34(6):462–75.
99. Alam SR, Shah ASV, Richards J, Lang NN, Barnes G, Joshi N, et al. Ultrasmall superparamagnetic particles of iron oxide in patients with acute myocardial infarction: early clinical experience. *Circ Cardiovasc Imaging*. 2012;5(5):559–65.
100. Alam SR, Stirrat C, Richards J, Mirsadraee S, Semple SIK, Tse G, et al. Vascular and plaque imaging with ultrasmall superparamagnetic particles of iron oxide. *J Cardiovasc Magn Reson*. 2015;17:83.
101. Burke C, Alexander Grant L, Goh V, Griffin N. The role of hepatocyte-specific contrast agents in hepatobiliary magnetic resonance imaging. *Semin Ultrasound CT MR*. 2013;34(1):44–53.
102. Fernandes JL, Storey P, da Silva JA, de Figueiredo GS, Kalaf JM, Coelho OR. Preliminary assessment of cardiac short term safety and efficacy of manganese chloride for cardiovascular magnetic resonance in humans. *J Cardiovasc Magn Reson*. 2011;13:6.
103. Thurnher S, Miller S, Schneider G, Ballarati C, Bongartz G, Herborn CU, et al. Diagnostic performance of gadobenate dimeglumine enhanced MR angiography of the iliofemoral and calf arteries: a large-scale multicenter trial. *Am J Roentgenol*. 2007;189(5):1223–37.
104. Camren GP, Wilson GJ, Bamra VR, Nguyen KQ, Hippe DS, Maki JH. A comparison between gadofosveset trisodium and gadobenate dimeglumine for steady state MRA of the thoracic vasculature. *Biomed Res Int*. 2014;2014:Article ID 625614, 6 pages.
105. Christie A, Chandramohan S, Roditi G. Comprehensive MRA of the lower limbs including high-resolution extended-phase infringuinal imaging with gadobenate dimeglumine: initial experience with inter-individual comparison to the blood-pool contrast agent gadofosveset trisodium. *Clin Radiol*. 2013;68(2):125–30.
106. Frydrychowicz A, Russe MF, Bock J, Stalder AF, Bley TA, Harloff A, et al. Comparison of gadofosveset trisodium and gadobenate dimeglumine during time-resolved thoracic MR angiography at 3T. *Acad Radiol*. 2010;17(11):1394–400.
107. Erb-Eigner K, Taupitz M, Asbach P. Equilibrium-phase MR angiography: comparison of unspecific extracellular and protein-binding gadolinium-based contrast media with respect to image quality. *Contrast Media Mol Imaging*. 2016;11(1):71–6.
108. Deray G, Rouviere O, Bacigalupo L, Maes B, Hannedouche T, Vrtovsnik F, et al. Safety of meglumine gadoterate (Gd-DOTA)-enhanced MRI compared to unenhanced MRI in patients with chronic kidney disease (RESCUE study). *Eur Radiol*. 2013;23(5):1250–9.
109. Ishiguchi T, Takahashi S. Safety of gadoterate meglumine (Gd-DOTA) as a contrast agent for magnetic resonance imaging: results of a post-marketing surveillance study in Japan. *Drugs R D*. 2010;10(3):133–45.
110. Kim RJ, Wu E, Rafael A, Chen EL, Parker MA, Simonetti O, et al. The use of contrast-enhanced magnetic resonance imaging to identify reversible myocardial dysfunction. *N Engl J Med*. 2000;343(20):1445–53.
111. Jerosch-Herold M, Kwong RY. Magnetic resonance imaging in the assessment of ventricular remodeling and viability. *Radiographics*. 2008;5(1):5–10.
112. Rudolph A, Messroghli D, Knobelsdorff-Brenkenhoff von F, Traber J, Schuler J, Wassmuth R, et al. Prospective, randomized comparison of gadopentetate and gadobutrol to assess chronic myocardial infarction applying cardiovascular magnetic resonance. *BMC Med Imaging*. 2015;15:55.
113. Heydari B, Jerosch-Herold M, Kwong RY. Assessment of myocardial ischemia with cardiovascular magnetic resonance. *Prog Cardiovasc Dis*. 2011;54(3):191–203.
114. Nagel E, Klein C, Paetsch I, Hettwer S, Schnackenburg B, Wegscheider K, et al. Magnetic resonance perfusion measurements for the noninvasive detection of coronary artery disease. *Circulation*. 2003;108(4):432–7.
115. Heydari B, Kwong RY, Jerosch-Herold M. Technical advances and clinical applications of quantitative myocardial blood flow imaging with cardiac MRI. *Prog Cardiovasc Dis*. 2015;57(6):615–22.